
Prisma Sains: Jurnal Pengkajian Ilmu dan Pembelajaran Matematika dan IPA IKIP Mataram
https://e-journal.undikma.ac.id/index.php/prismasains/index
e-mail: prismasains.pkpsm@gmail.com

October 2025. Vol. 13, No. 4
p-ISSN: 2338-4530
e-ISSN: 2540-7899
pp. 1053–1065

A ZE25A-O3 Sensor-Based Solution for Continuous Ozone Level Measurement in LINAC Environments

[1*]Nur Khasanah, [2]Lalu Sahrul Hudha, [3]Jamiluddin, [1]Nevi Ernita, [4]Bunawas, [5]I Wayan Ari M, [5]Rinarto Subroto

[1]*Physics Education Department, Faculty of Tarbiyah and Teacher Training, Universitas Islam Negeri Mataram, Jl GajahMada No.100, Jempong Baru, Mataram, Nusa Tenggara Barat, Indonesia
[2]Physics Department, Faculty of Mathematical and Science, University of Mataram
[3]Social Studies Education Department, Faculty of Tarbiyah and Teacher Training, Universitas Islam Negeri Mataram
[4]PT. Nuklir Teknologi Indonesia, Tangerang Selatan, Banten, Indonesia
[5]Radiotherapy Installation, RSUD Provinsi NTB

*Corresponding Author e-mail: nurkhasanah@uinmataram.ac.id

Received: June 2025; Revised: September 2025; Published: October 2025

Abstract

Ozone (O_3) generated during LINAC operation can accumulate indoors and pose respiratory risks, yet many facilities lack continuous monitoring. We designed and validated a low-cost, electrochemical sensor platform—ZE25A-O_3 integrated with an Arduino Mega, on-board logging, and a Nextion HMI—for real-time surveillance in a LINAC suite. The sensor was calibrated at 24 °C and 40% RH against 0.5–1.5 ppm standards, yielding slope = 1.045, intercept = −0.04067 ppm, R^2 = 0.99984, and RMSE = 9.39 ppb, supporting reliable low-ppb quantification. Time series were aggregated into 30-min bins with centered 1-h rolling means to extract diurnal structure while suppressing short-term fluctuations. Field measurements showed a 20–30 ppb background with intermittent spikes exceeding 100 ppb (peaks ~150 ppb). A reproducible daily pattern emerged: late-morning minima (~20–21 ppb) followed by evening enhancement (~26–28 ppb), consistent with ventilation and operational schedule. Average conditions were below the Indonesian workplace limit of 100 ppb, but episodic exceedances motivate real-time alerts and ventilation management. This work demonstrates a practical approach for continuous exposure assessment and data-informed environmental control in radiotherapy facilities.

Keywords: Ozone; LINAC; electrochemical; ZE25A-O3

How to Cite: Khasanah, N., Hudha, L. S., Jamiluddin, J., Ernita, N., Bunawas, B., M, I. W. A., & Subroto, R. (2025). A ZE25A-O3 Sensor-Based Solution for Continuous Ozone Level Measurement in LINAC Environments. *Prisma Sains : Jurnal Pengkajian Ilmu Dan Pembelajaran Matematika Dan IPA IKIP Mataram*, *13*(4), 1053–1065. https://doi.org/10.33394/j-ps.v13i4.16540

https://doi.org/10.33394/j-ps.v13i4.16540

INTRODUCTION

Radiotherapy is one of the most common treatments for cancer, using ionizing radiation to target and destroy cancer cells while minimizing damage to surrounding healthy tissue (Dev & Maria, 2024; Vaidya, 2021). The Linear Accelerator (LINAC) plays a crucial role in this process by generating high-energy photon and electron beams, which are used to treat deep-seated tumors(Santamaria et al., 2022) and cancers near the skin surface (Kutsaev et al., 2021). However, one of the products of operating LINAC in electron mode is the generation of ozone (O_3) (McCallum-Hee et al., 2025; Vidmar & Stalder, 2008), which can accumulate in enclosed spaces such as treatment rooms (Khasanah et al., 2024). Ozone is a toxic gas (Weschler, 2000), and while it protects the earth from harmful UV radiation in the atmosphere, elevated concentrations in confined environments can lead to health (Adler & Severnini, 2023; Gao et al., 2022; Guan et al., 2022; Ma et al., 2020; Niu et al., 2018; Nuvolone et al., 2018; Salonen et al., 2018), including respiratory issues for patients and medical personal. Based on Regulation of the Minister of Health of the Republic of Indonesia No. 70 of 2016 concerning Health Standards and Requirements in Industrial Workplaces, one of these standards is the limit value for chemicals in the workplace, which is 0.1 ppm or 100 ppb (Permenkes, 2016).

Studies have shown that LINAC operation can produce significant levels of ozone, particularly during high-energy electron treatments (Barshan et al., 2020; Cleland & Galloway, 2015; Dubey et al., 2009; Hara et al., 2022; Mishra et al., 2018). Research by Lee et al. (2016) revealed that ozone concentration in LINAC rooms can reach up to double the background levels during operation and takes over 10 minutes to dissipate after the treatment ends (Lee et al., 2016). Research conducted by Hara et al. (2022) measured the ozone concentration in the LINAC room using the UV absorption method and ozone analyzer. This research showed that the maximum ozone concentration obtained was only 0.006 ppm when irradiated at a dose rate of 2,400 MU/minute (Hara et al., 2022). Khasanah et al. (2024) conducted research to measure ozone concentrations in the LINAC control room and patient waiting room. Ozone concentration measurements were performed using an ozone meter. The maximum concentration of ozone in the LINAC patient waiting room was obtained at an energy of 12 MeV of 6.6 ppb and in the LINAC control room it was obtained at an energy of 12 MeV of 8.3 ppb (Khasanah et al., 2024). Currently developed ozone concentration measurement systems include semiconductor-based sensors(Demin et al., 2008; Gómez-Suárez et al., 2022; Wu et al., 2024), electrochemical sensors(Afshar-Mohajer et al., 2018; Badura et al., 2022; Pang et al., 2017), and UV photometric sensors (Barreto et al., 2022; Borrego et al., 2016; Cross et al., 2017; Mueller et al., 2017; Signorini et al., 2017; Spinelle et al., 2015; Sun et al., 2016). Each of these ozone concentration measurement systems has its own advantages and disadvantages. Despite these findings, many LINAC installations, lack a ozone monitoring system. This presents a risk, as sudden spikes in ozone concentration may go unnoticed, potentially endangering those within the room. Therefore, this research will develop a ozone gas measurement system inside a LINAC radiotherapy room.

The objective of this research is to design and implement ozone concentration measurement and monitoring system in the LINAC. The system enables continuous monitoring and provides immediate alerts when ozone levels exceed safety thresholds. Electrochemical sensors are integrated into the system to detect ozone accurately, with data accessible remotely via mobile devices and dashboards. This ensures that the environment remains safe for both staff and patients during radiotherapy sessions. This research contributes to the development of safer radiation therapy environments by introducing a monitoring system that not only detects and records ozone levels but also enables long-term data collection for further analysis and evaluation of ventilation systems. The findings from this study will enhance safety protocols and provide valuable insights into managing ozone levels in radiotherapy facilities.

METHOD

System overview & requirements

This research employs a Research and Development (R&D) approach aimed at designing, building, and implementing a real-time ozone concentration measurement system for the LINAC radiotherapy. The system is designed to provide data to monitor ozone levels, which can be accessed by medical staff and ensure the safety of both patients and personnel working in the radiotherapy facility. The research was conducted at the LINAC radiotherapy room. The development model followed a prototyping approach that includes several stages: identifying objectives and needs, selecting the measurement methods, choosing hardware components, system design, software development, testing and validation, implementation, and system performance evaluation. This step-by-step approach ensures that the final system meets the requirements for ozone concentration monitoring in a radiotherapy setting.

Hardware & electronics

The ozone concentration measurement system is composed of several subsystems. Sensor Subsystem: This includes an ozone sensor (ZE25A-O3) to measure ozone concentration in the LINAC room. Output Subsystem: The output subsystem includes a Nextion TFT LCD for displaying real-time measurements, and a data logger for storing the results. Power Subsystem: This powers the entire system, ensuring consistent operation during measurements. Air Pump Subsystem: This ensures that air samples are effectively captured for accurate ozone level measurements.

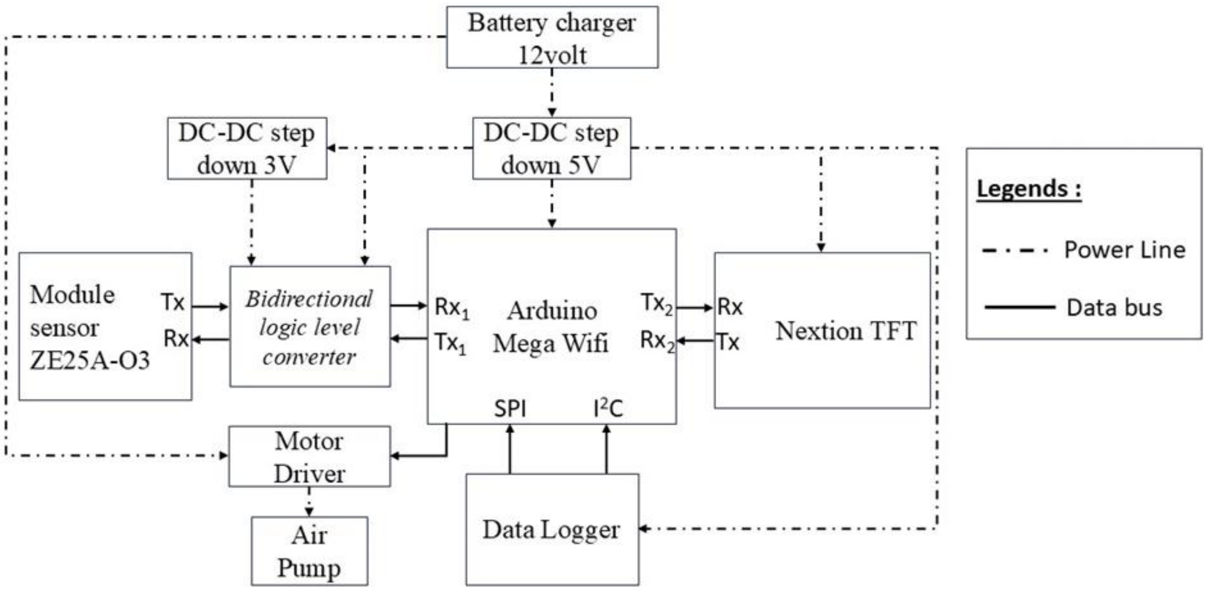

Figure 1 Block Diagram of the Ozone Measurement and Monitoring System

PIN1	Reserved
PIN2	Reserved
PIN3	GND
PIN4	Vin (input 3.7V~5.5V)
PIN5	UART (RXD) 0~3.0V Data input
PIN6	UART (TXD) 0~3.0V Data output
PIN7	Reserved

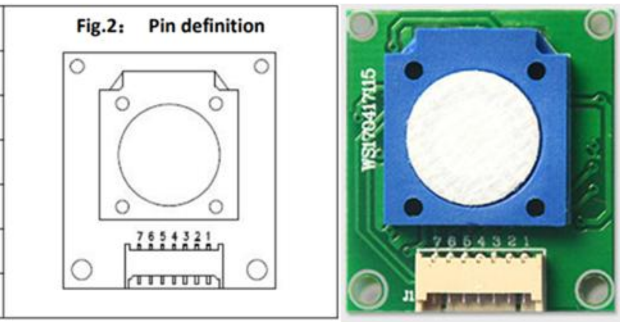

Figure 2. Sensor specification of ZE25A-O3(Zhengzhou Winsen Electronics TechnologyCo., 2021)

The ZE25A-O3 is an ozone (O_3) gas sensor module with a detection range of 0–2 ppm and a resolution of 0.001 ppm. It communicates via UART at a 3 V logic level and operates from 3.7–5.5 V (no reverse-voltage protection). Typical timings are a warm-up time ≤3 minutes, response time ≤90 seconds, and resume time ≤90 seconds. It functions over −10 to 55 °C and 15–90% RH (non-condensing), with a storage temperature of −20 to 55 °C. The stated service life is 2 years in air.

To ensure safe and reliable serial communication between the ZE25A-O3 module (3 V logic) and the Arduino Mega (5 V logic), we employ a bidirectional MOSFET-based level-shifting interface(Yang & Hongmei Lu, 2012), shown in Figure 3. The translator implements one channel per UART direction: Q1 conditions the sensor's TX line to the Mega's RX input, and Q2 conditions the Mega's TX line to the sensor's RX input. Each side is weakly pulled up to its native rail through 10 kΩ resistors (R1 and R3 to 3 V; R2 and R4 to 5 V). In the idle state, both lines sit high at their respective voltages.

Figure 3 Bidirectional logic level conventer

This topology preserves signal integrity for standard UART baud rates, provides true electrical isolation between the 3 V and 5 V logic domains, and avoids the asymmetry and leakage issues of simple resistor dividers. Consequently, the interface in Figure 3 offers a compact, robust solution for bidirectional level conversion between the ZE25A-O3 sensor and the Arduino Mega's serial ports in continuous ozone monitoring applications.

Calibration & validation

The system was calibrated using standard procedure by Zhenzhou Winsen Electronics Technology. Calibration data, including system sensitivity, resolution, and repeatability, was gathered to ensure the accuracy of the ozone measurement system. Calibration of the ZE25A-O_3 electrochemical ozone sensor was conducted at 24 °C and 40%RH using certified O_3 gas standards at three setpoints (0.5, 1.0, and 1.5 ppm). For each setpoint, the stabilized sensor output (ppm) was recorded and paired with the reference concentration (ppm).

Study site & sampling design

Ozone concentration data was collected inside the LINAC room by placing the system at a points in proximity to the treatment area. The system recorded real time data, capturing variables such as timing and ozone concentration.

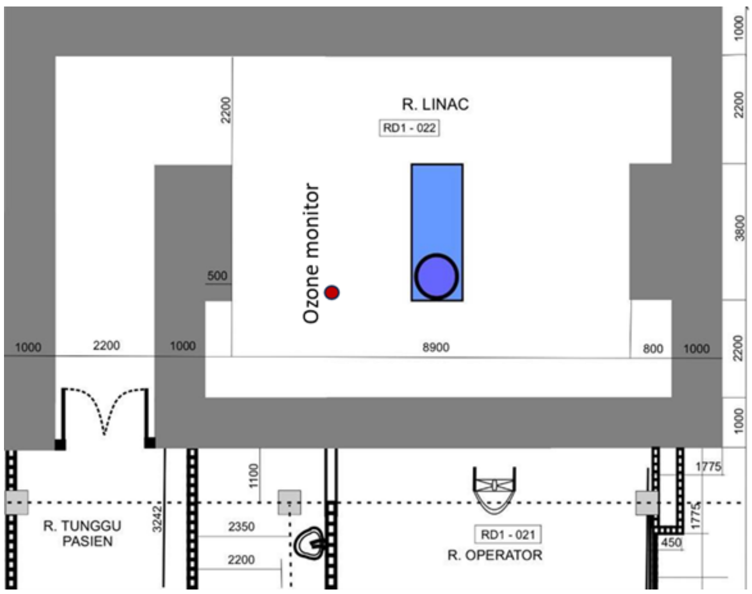

Figure 4 Floor plan of LINAC room with sensor locations

Data analysis

Data was analyzed by comparing measured ozone levels with background concentrations. The calibration factor was applied to correct the measured values. The final ozone concentration data was presented in parts per billion (ppb), and results were compared to the threshold limit for workplace safety, set at 100 ppb according to Indonesian regulations. Time stamps recorded as HH:MM:SS were converted to absolute time by detecting day rollovers and indexing observations from Day-1 09:00:15 through Day-3 12:04:00. Ozone concentrations (ZE25A-O_3; ppb) were then aggregated into 30-minute bins (top-of-bin alignment). For each bin we computed the mean, median, standard deviation, and count. To highlight the within-day pattern while suppressing high-frequency fluctuations, we overlaid a centered 1-hour rolling mean on the 30-minute series (i.e., a two-point rolling average on the 30-minute means). Daily (diurnal) profiles were derived by averaging the concentration at each hour-of-day (0–23) across all days (“aggregate diurnal”), and separately by day (“per-day diurnal”). Where helpful for visual interpretation, the y-axis was restricted to 20–30 ppb

RESULTS AND DISCUSSION

This study successfully developed a real-time ozone concentration measurement and monitoring system for the Linear Accelerator (LINAC) radiotherapy. The system was built using an electrochemical ozone sensor (ZE25A-O_3), a microcontroller (Arduino Mega), and a monitoring platform. The results from the system testing and ozone monitoring revealed significant insights into ozone concentration during LINAC operations. The system was validated through calibration, testing, and design optimization to ensure accurate performance in the LINAC environment.

System Development and Design

The hardware consists of an ozone sensor (ZE25A-O_3), a microcontroller (Arduino Mega), Data logger module, Display unit based on Nextion TFT. The sensor module communicates with the microcontroller through a Serial UART interface.

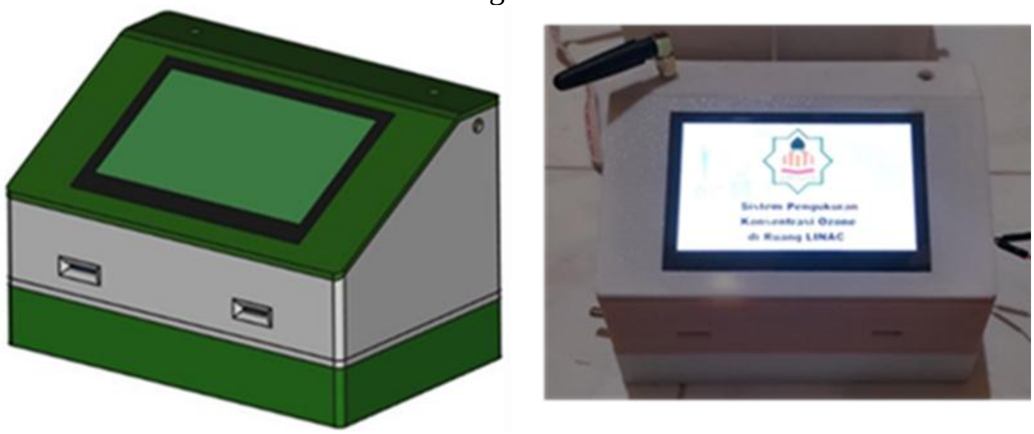

Figure 5 Implementation of the Ozone Concentration Measurement and Monitoring System

Due to different voltage levels between the sensor (3V) and the microcontroller (5V), a level shifter circuit was incorporated to ensure accurate communication between the components.

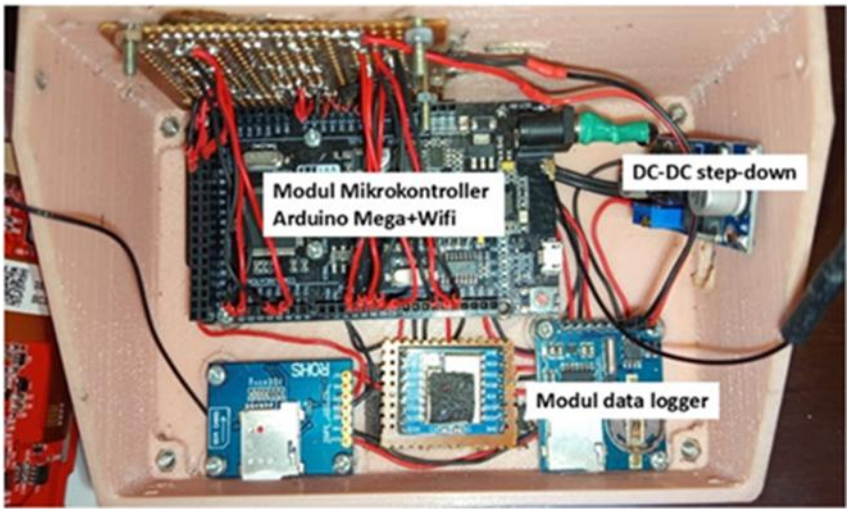

Figure 6 Integrated Hardware of the Ozone Concentration Measurement System

The power management system includes a 12V adapter and a 2000mAh lithium battery to maintain continuous operation, even during power interruptions. The power system also supplies the sensors and the microcontroller with a stable power source.

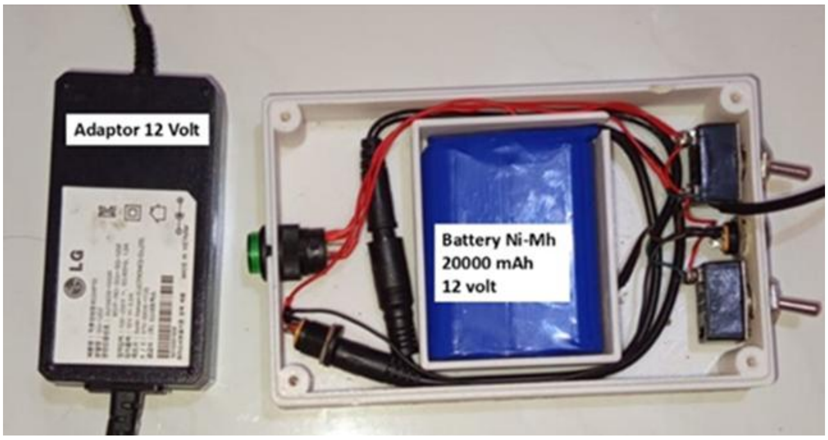

Figure 7 Power System of the Ozone Measurement System

Calibration and accuracy of reference

The ZE25A-O_3 sensor was calibrated at Zhengzhou Winsen Electronics Technology under controlled conditions (24 °C, 40 %RH) using certified ozone standards at 0.5, 1.0, and 1.5 ppm. A linear forward model $y_{sensor} = a + b_{x_{ref.}}$ fitted to these points yielded an intercept of −0.04067±0.01434 ppm and a slope of 1.045±0.013281.045 (ppm/ppm), with excellent goodness of fit (R^2=0.99984) and root-mean-square error of 0.00939 ppm (≈ 9.39 ppb), as shown in Figure 8.

The slope greater than unity indicates sensor sensitivity about 4.5 % higher than the reference, whereas the negative intercept (≈ −40.7 ppb) implies a downward offset that becomes influential when extrapolating toward low concentrations. Accordingly, calibrated ozone concentrations were computed from raw sensor readings using the inverse mapping which is appropriate for reporting in either ppm or ppb. Taken together, the tight fit, high R^2, and low RMSE indicate that this calibration is adequate for accurate, routine monitoring of ozone concentration in the LINAC environment, enabling hourly averages and diurnal profiles to be quantified with confidence.

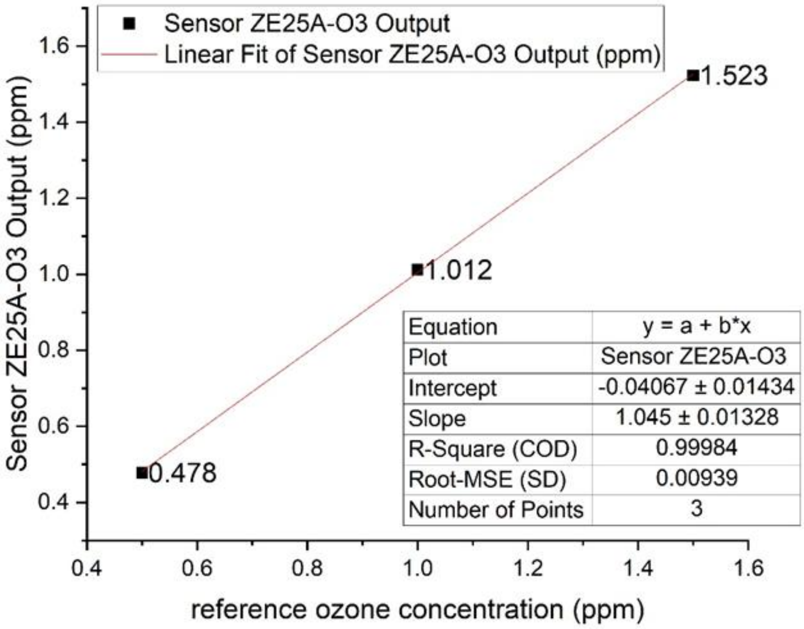

Figure 8 Calibration curve of the ZE25A-O_3 sensor

Human-Machine Interface (HMI)

The system includes an HMI display using a Nextion TFT LCD screen, which provides real-time feedback to users located near the LINAC room. The display shows both numerical and graphical representations of ozone concentration, making it easier for operators to monitor environmental conditions. The system also features an alert mechanism, such as a buzzer, that is activated when the ozone levels approach the upper safety threshold. This provides an immediate local warning to personnel in the facility. Figure 9 shows the HMI performance.

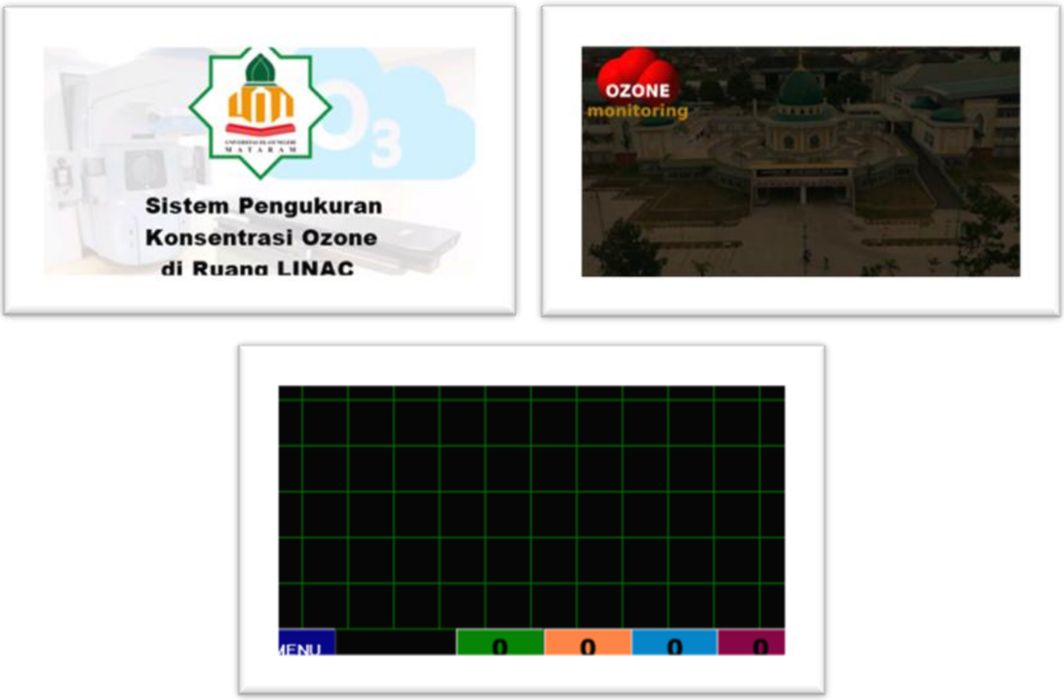

Figure 9 HMI performance

Ozone Concentration Measurements

Overview of the time series (Figure 10)

The raw real-time series reveals a highly intermittent signal with sharp excursions superimposed on a relatively stable baseline. Instantaneous values periodically rise above 100 ppb, with the largest spikes approaching ~150 ppb, whereas the smoothed trajectories (1-h and 2-h rolling means) remain in a much narrower band of ~20–30 ppb. This contrast indicates short-duration events (likely linked to equipment operation, occupancy, or transient airflows) riding on top of a slow-varying background determined by the room's ventilation and routine activity. Two features stand out. First, long plateaus near ~20–22 ppb are visible around midday/early afternoon, suggesting a daily minimum in the underlying background. Second, the rolling means gradually increase toward late afternoon and evening, consistent with a diurnal buildup phase. The 2-h curve is, as expected, smoother and emphasizes the low-frequency background, while the 1-h curve tracks sub-daily variability more closely. The baseline likely reflects room ventilation set-points and outdoor/indoor exchange, while the high peaks represent episodic sources (e.g., machine cycles, cleaning or sterilization steps, or brief stagnation periods). Because the rolling means do not follow the spikes, these events are short compared to one hour.

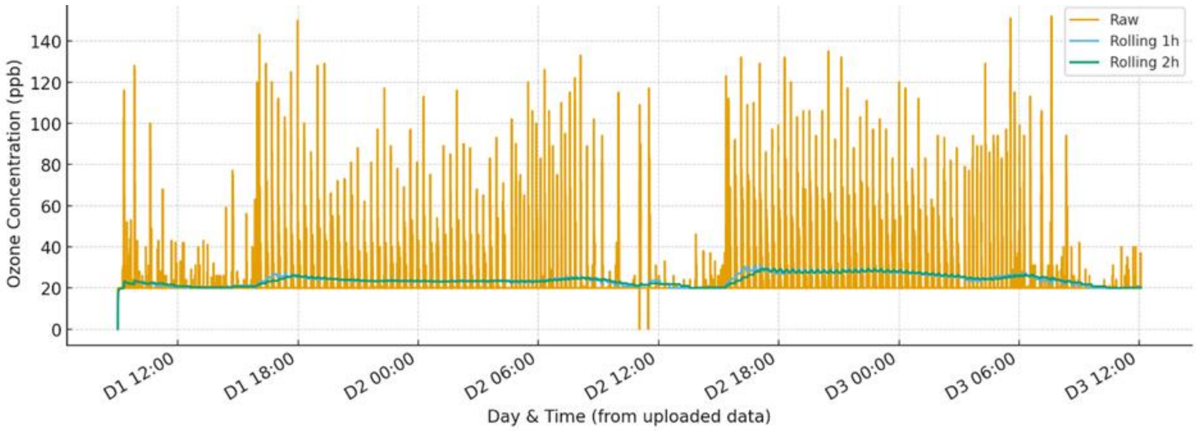

Figure 10 Ozone Concentration in LINAC Room

Half-hour averages to reduce short-term noise (Figure 11)

Aggregating to 30-min bins reduces the influence of bursts and clarifies the low-frequency trend. The half-hour means typically sit between ~20 and ~30 ppb. A "pattern" line (2-h smoothing) highlights a structured evolution across the day: Means hover around ~24–25 ppb with modest variability at pre-dawn to morning (~00:00–08:30), a progressive decline reaches the daily minimum near ~20–21 ppb at late morning to early afternoon (~09:00–14:00), and the mean rises sharply, stabilizing around ~25–28 ppb through the evening and early night (~15:00 onward). The half-hour means reinforce the presence of a robust cycle: lower background during midday/early afternoon and higher levels during late afternoon/evening. This can arise from (i) HVAC scheduling (e.g., daytime dilution vs. evening recirculation), (ii) in-room activities that intensify later in the day, or (iii) outdoor-to-indoor transport interacting with photochemical production and decay. While raw ozone often declines indoors due to surface losses and reactions, late-day rises in indoor measurements can occur if ventilation settings change or if indoor sources/processes are active.

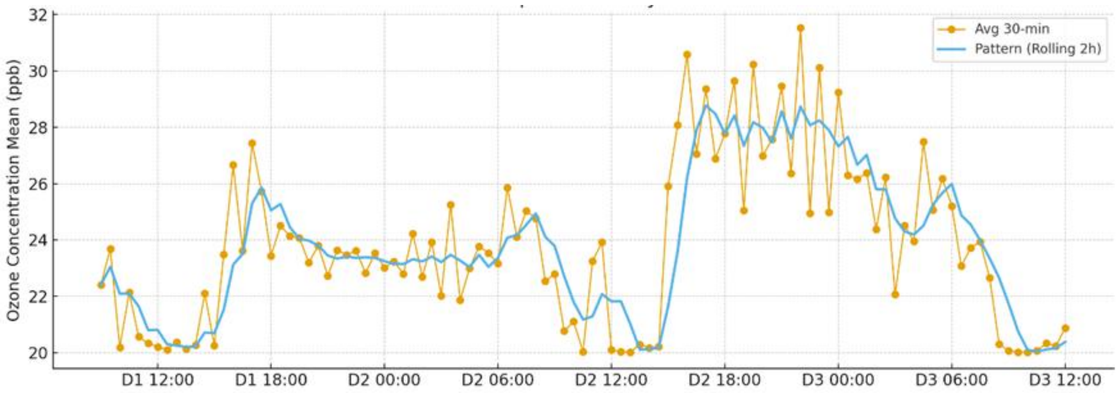

Figure 11 30-Minute Average Ozone with Pattern Line (Rolling 2h)

Composite daily pattern across days (Figure 12)

To reveal the typical daily cycle independent of day-to-day events, we formed a composite by averaging all data by time-of-day in 30-min bins. The composite mean shows a gentle pre-dawn plateau (~24–25 ppb), a late-morning/early-afternoon trough at ~20–21 ppb (≈ 12:00–14:00), and a pronounced afternoon ramp beginning ~15:00 and peaking into the evening around ~26–28 ppb. This composite confirms that the diurnal structure is not an artifact of one particular day: the sequence "plateau → midday minimum → evening rise" is persistent. The composite pattern is consistent with a background controlled by ventilation strategy and routine operations. The timing of the minimum suggests maximum dilution or removal during the core work window, followed by reduced dilution or enhanced indoor processes later in the day.

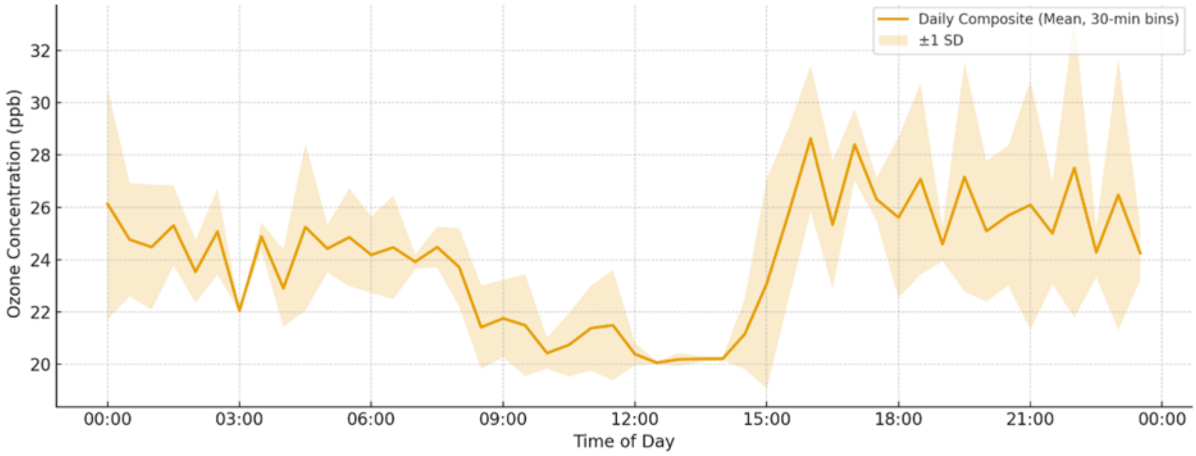

Figure 12 Composite Daily Pattern of Ozone

Sensitivity of the "pattern" to smoothing scale (Figure 13)

Replacing the 2-h smoother with a 1-h rolling window increases responsiveness to short-lived shifts while preserving the daily envelope. The 1-h pattern line lies close to the 30-min means during transitions (e.g., the afternoon ramp), but remains smooth enough to suppress spike-level noise. This confirms the diurnal signal's robustness across reasonable smoothing choices: both windows identify the same midday minimum and evening enhancement, with only minor differences in the sharpness of transitions

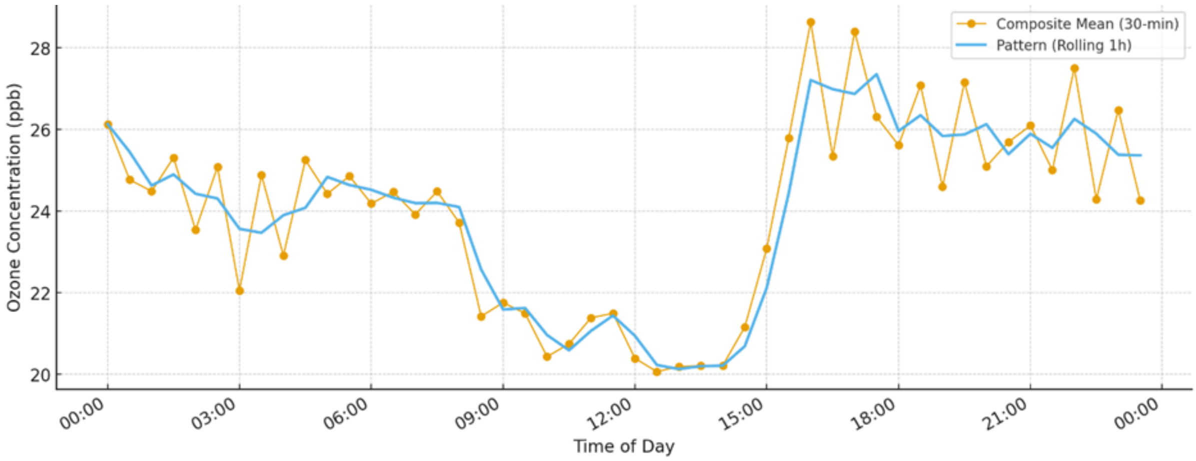

Figure 13 Composite Daily Pattern of Ozone (30 min bins) with 1h Pattern

CONCLUSION

This research demonstrates the feasibility and utility of a low-cost, electrochemical sensor–based system for continuous ozone surveillance in LINAC environments. The prototype—built around the ZE25A-O_3 sensor, Arduino Mega, on-board data logging, and a Nextion HMI—achieved excellent calibration performance under controlled conditions (slope ≈ 1.045, intercept ≈ −0.0407 ppm, R^2 ≈ 0.9998; RMSE ≈ 9.39 ppb), supporting reliable quantification in the low-ppb regime relevant to occupational safety. Deployed measurements revealed a stable background of ~20–30 ppb with intermittent short-duration excursions, some exceeding 100 ppb, and a reproducible diurnal structure characterized by a late-morning minimum (~20–21 ppb) and evening enhancement (~26–28 ppb). These findings indicate that while average conditions remain below the Indonesian threshold of 100 ppb, transient peaks can breach this limit, underscoring the need for real-time alerts and ventilation management tied to clinical workflow. Collectively, the results validate the system as a practical tool for continuous exposure assessment, incident detection, and facilities optimization in radiotherapy suites. Future work should extend monitoring to multi-point networks, perform longer-term co-location against reference UV photometric analyzers, and integrate automated feedback to HVAC controls to mitigate episodic spikes. Such enhancements would further strengthen patient and staff protection while enabling data-driven environmental stewardship in LINAC operations.

RECOMMENDATION

Further research can be focused on developing a system that is more integrated with the environmental control system in the LINAC room, so that it can not only monitor but also regulate ozone levels.

FUNDING INFORMATION

Funding for research implementation and article publication costs are financed by BOPTN UIN Mataram. This is done to fulfill the Tridharma duties in the field of research and for the needs of the lecturer's performance load.

AUTHOR CONTRIBUTIONS STATEMENT

Name of Author	C	M	So	Va	Fo	I	R	D	O	E	Vi	Su	P	Fu
Nur Khasanah	✓	✓		✓	✓	✓		✓	✓	✓			✓	✓
Lalu Sahrul Hudha		✓	✓			✓		✓	✓	✓	✓	✓		
Jamiluddin			✓	✓			✓			✓	✓		✓	✓
Nevi Ernita							✓		✓	✓			✓	✓
Bunawas	✓	✓						✓				✓		
I Wayan Ari M							✓	✓				✓	✓	
Rinarto Subroto							✓	✓				✓	✓	

DATA AVAILABILITY

All data necessary to support the conclusions of this study are available upon reasonable request from the corresponding author,NK.

REFERENCES

Adler, D., & Severnini, E. (2023). Timing matters: Intra-day shifts of economic activity and ambient ozone concentrations. *Journal of Public Economics*, *223*. https://doi.org/10.1016/j.jpubeco.2023.104905

Afshar-Mohajer, N., Zuidema, C., Sousan, S., Hallett, L., Tatum, M., Rule, A. M., Thomas, G., Peters, T. M., & Koehler, K. (2018). Evaluation of low-cost electro-chemical sensors for environmental monitoring of ozone, nitrogen dioxide, and carbon monoxide. *Journal of Occupational and Environmental Hygiene*, *15*(2), 87–98. https://doi.org/10.1080/15459624.2017.1388918

Badura, M., Batog, P., Drzeniecka-Osiadacz, A., & Modzel, P. (2022). Low- and Medium-Cost Sensors for Tropospheric Ozone Monitoring—Results of an Evaluation Study in Wrocław, Poland. *Atmosphere*, *13*(4), 542. https://doi.org/10.3390/atmos13040542

Barreto, D. N., Silva, W. R., Mizaikoff, B., & da Silveira Petruci, J. F. (2022). Monitoring Ozone Using Portable Substrate-Integrated Hollow Waveguide-Based Absorbance Sensors in the Ultraviolet Range. *ACS Measurement Science Au*, *2*(1), 39–45. https://doi.org/10.1021/acsmeasuresciau.1c00028

Barshan, S., Pazirandeh, A., & Jahanfarnia, G. (2020). Measurement of ozone produced by 10 MeV electron accelerator Yazd in various currents. *Journal of Instrumentation*, *15*(1). https://doi.org/10.1088/1748-0221/15/01/P01004

Borrego, C., Costa, A. M., Ginja, J., Amorim, M., Coutinho, M., Karatzas, K., Sioumis, T., Katsifarakis, N., Konstantinidis, K., De Vito, S., Esposito, E., Smith, P., André, N., Gérard, P., Francis, L. A., Castell, N., Schneider, P., Viana, M., Minguillón, M. C., … Penza, M. (2016). Assessment of air quality microsensors versus reference methods: The EuNetAir joint exercise. *Atmospheric Environment*, *147*, 246–263. https://doi.org/10.1016/j.atmosenv.2016.09.050

Cleland, M. R., & Galloway, R. A. (2015). Ozone Generation in Air during Electron Beam Processing. *Physics Procedia*, *66*, 586–594. https://doi.org/https://doi.org/10.1016/j.phpro.2015.05.078

Cross, E. S., Williams, L. R., Lewis, D. K., Magoon, G. R., Onasch, T. B., Kaminsky, M. L., Worsnop, D. R., & Jayne, J. T. (2017). Use of electrochemical sensors for measurement of air pollution: Correcting interference response and validating measurements. *Atmospheric Measurement Techniques*, *10*(9), 3575–3588. https://doi.org/10.5194/amt-10-3575-2017

Demin, V. S., Krasovskii, A. N., Lyudchik, A. M., Pokatashkin, V. I., Grigorishin, I. L., & Kudanovich, O. N. (2008). Measurement of ozone over a wide range of concentrations using semiconductor NiO gas sensors. *Measurement Techniques*, *51*(9), 1038–1044. https://doi.org/10.1007/s11018-008-9149-3

Dev, D., & Maria, E. Malafi. (2024). The Lives Saved: A Literature Review on the Role of Radiotherapy Improving Prognosis in Cancer Patients. *Journal of Quality in Health Care & Economics*, *7*(1), 1–3. https://doi.org/10.23880/jqhe-16000360

Dubey, P., Sawatkar, A. R., Sathe, A. P., Sarma, K. S. S., & Soundararajan, S. (2009). GENERATION OF OZONE AND SAFETY ASPECTS IN AN ACCELERATOR FACILITY OF BARC. *Proceedings of the DAE-BRNS Indian Particle Accelerator Conference*.

Gao, Q., Zang, E., Bi, J., Dubrow, R., Lowe, S. R., Chen, H., Zeng, Y., Shi, L., & Chen, K. (2022). Long-term ozone exposure and cognitive impairment among Chinese older adults: A cohort study. *Environment International*, *160*. https://doi.org/10.1016/j.envint.2021.107072

Gómez-Suárez, J., Arroyo, P., Cerrato-Álvarez, M., Hontañón, E., Masa, S., Menini, P., Presmanes, L., Alfonso, R., Pinilla-Gil, E., & Lozano, J. (2022). Development and Field Validation of Low-Cost Metal Oxide Nanosensors for Tropospheric Ozone Monitoring in Rural Areas. *Chemosensors*, *10*(11), 478. https://doi.org/10.3390/chemosensors10110478

Guan, Y., Xiao, Y., Chu, C., Zhang, N., & Yu, L. (2022). Trends and characteristics of ozone and nitrogen dioxide related health impacts in Chinese cities. *Ecotoxicology and Environmental Safety*, *241*. https://doi.org/10.1016/j.ecoenv.2022.113808

Hara, N., Oobuchi, J., Isobe, A., Sugimoto, S., Takatsu, J., & Sasai, K. (2022). Generation of ozone during irradiation using medical linear accelerators: an experimental study. *Radiation Oncology*, *17*(1). https://doi.org/10.1186/s13014-022-02005-6

Khasanah, N., Raehanah, Bunawas, M, I. W. A., Subroto, R., H, L. S., A, P. P., & Ulfariah, D. (2024). Measurement and Risk Analysis of Ozone (O3) Concentrations in the 9 MeV and 12 MeV Electron Mode LINAC. *Jurnal Penelitian Pendidikan IPA*, *10*(2), 757–763. https://doi.org/10.29303/jppipa.v10i2.5347

Kutsaev, S. V, Boucher, S., Mustapha, B., & Sheng, K. (2021). Novel technologies for Linac-based radiotherapy. In N. J. Cherepy, M. Fiederle, & R. B. James (Eds.), *Hard X-Ray, Gamma-Ray, and Neutron Detector Physics XXIII* (Vol. 11838, p. 118380U). SPIE. https://doi.org/10.1117/12.2595707

Lee, J., Lee, H.-Y., Im, I.-C., & Yu, Y.-S. (2016). Variation of Indoor Average Ozone Concentration within the Radiation Therapy Room by High Energy Radiation. *Journal of the Korean Society of Radiology*, *10*(3), 171–180. https://doi.org/10.7742/jksr.2016.10.3.171

Ma, R., Ban, J., Wang, Q., & Li, T. (2020). Statistical spatial-temporal modeling of ambient ozone exposure for environmental epidemiology studies: A review. In *Science of the Total Environment* (Vol. 701). Elsevier B.V. https://doi.org/10.1016/j.scitotenv.2019.134463

McCallum-Hee, B. I., Ibrahim, M., Mukwada, G., Rowshanfarzad, P., Dass, J., Dewitt, J., Parin, R., Withey, G., & Alkhatib, Z. (2025). Commissioning and clinical implementation of low dose dual-field rotational TSET. *Journal of Applied Clinical Medical Physics*, *26*(7). https://doi.org/10.1002/acm2.70180

Mishra, A. S., Verma, V. P., Choudhary, R. S., Goswami, S. G., Petwal, V. C., & Dwivedi, J. (2018). *Ozone concentration study using 10 MeV electron beam accelerator*. https://inis.iaea.org/search/search.aspx?orig_q=RN:49082934

Mueller, M., Meyer, J., & Hueglin, C. (2017). Design of an ozone and nitrogen dioxide sensor unit and its long-Term operation within a sensor network in the city of Zurich. *Atmospheric Measurement Techniques*, *10*(10), 3783–3799. https://doi.org/10.5194/amt-10-3783-2017

Niu, Y., Cai, J., Xia, Y., Yu, H., Chen, R., Lin, Z., Liu, C., Chen, C., Wang, W., Peng, L., Xia, X., Fu, Q., & Kan, H. (2018). Estimation of personal ozone exposure using ambient concentrations and influencing factors. *Environment International*, *117*, 237–242. https://doi.org/10.1016/j.envint.2018.05.017

Nuvolone, D., Petri, D., & Voller, F. (2018). The effects of ozone on human health. *Environmental Science and Pollution Research*, *25*(9), 8074–8088. https://doi.org/10.1007/s11356-017-9239-3

Pang, X., Shaw, M. D., Lewis, A. C., Carpenter, L. J., & Batchellier, T. (2017). Electrochemical ozone sensors: A miniaturised alternative for ozone measurements in laboratory experiments and air-quality monitoring. *Sensors and Actuators B: Chemical*, *240*, 829–837. https://doi.org/10.1016/j.snb.2016.09.020

Permenkes. (2016). *PERATURAN MENTERI KESEHATAN REPUBLIK INDONESIA*.

Salonen, H., Salthammer, T., & Morawska, L. (2018). Human exposure to ozone in school and office indoor environments. In *Environment International* (Vol. 119, pp. 503–514). Elsevier Ltd. https://doi.org/10.1016/j.envint.2018.07.012

Santamaria, V., Villarreta, K., & Solano, M. (2022). Dosimetric tests using the Step & Shoot technique for future implementation of IMRT with LINAC device at the ION. *2022 IEEE Central America and Panama Student Conference (CONESCAPAN)*, 1–5. https://doi.org/10.1109/CONESCAPAN56456.2022.9959394

Signorini, M. ., Kotsev, A. ., Gerboles, M. ., & Spinelle, L. . (2017). *Evaluation of low-cost sensors for air pollution monitoring effect of gaseous interfering compounds and meteorological conditions*. Publications Office.

Spinelle, L., Gerboles, M., Villani, M. G., Aleixandre, M., & Bonavitacola, F. (2015). Field calibration of a cluster of low-cost available sensors for air quality monitoring. Part A: Ozone and nitrogen dioxide. *Sensors and Actuators, B: Chemical*, *215*, 249–257. https://doi.org/10.1016/j.snb.2015.03.031

Sun, L., Wong, K. C., Wei, P., Ye, S., Huang, H., Yang, F., Westerdahl, D., Louie, P. K. K., Luk, C. W. Y., & Ning, Z. (2016). Development and application of a next generation air sensor network for the Hong Kong marathon 2015 air quality monitoring. *Sensors (Switzerland)*, *16*(2). https://doi.org/10.3390/s16020211

Vaidya, J. S. (2021). *Principles of cancer treatment by radiotherapy*. *39*(4). https://doi.org/https://doi.org/10.1016/j.mpsur.2021.02.002

Vidmar, R. J., & Stalder, K. R. (2008). Electron-beam generated air plasma: Ozone and electron density measurements. *2008 IEEE 35th International Conference on Plasma Science*, 1–1. https://doi.org/10.1109/PLASMA.2008.4590950

Weschler, C. J. (2000). Ozone in Indoor Environments: Concentration and Chemistry. *Indoor Air*, *10*, 269–288. http://journals.111unksgaard.dk/indoornir

Wu, C.-H., Lin, W.-Y., Kumar, U., Deng, Z.-Y., Lo, K. Y., & Chen, K.-L. (2024). Enhancing Ozone Gas Sensor Performance with Polypyrrole-Coated Metal-Oxide Semiconductors. *2024 IEEE SENSORS*, 1–4. https://doi.org/10.1109/SENSORS60989.2024.10785217

Yang, B., & Hongmei Lu. (2012). The key issues of dual-supply logic level conversion. *2012 24th Chinese Control and Decision Conference (CCDC)*, 3217–3221. https://doi.org/10.1109/CCDC.2012.6244509

Zhengzhou Winsen Electronics TechnologyCo., L. (2021). *Electrochemical Ozone Detection Module User's Manual*. www.winsen-sensor.com